Analysis and Mitigation of Resonance Propagation in Grid-Connected and Islanding Microgrids

Jinwei He, Yun Wei Li, *Senior Member, IEEE*, Ruiqi Wang, and Chenghui Zhang

***Abstract*—The application of underground cables and shunt capacitor banks may introduce power distribution system resonances. In this paper, the impacts of voltage-controlled and current-controlled distributed generation (DG) units to microgrid resonance propagation are compared. It can be seen that a conventional voltage-controlled DG unit with an *LC* filter has a short-circuit feature at the selected harmonic frequencies, while a current-controlled DG unit presents an open-circuit characteristic. Due to different behaviors at harmonic frequencies, specific harmonic mitigation methods shall be developed for current-controlled and voltage-controlled DG units, respectively. This paper also focuses on developing a voltage-controlled DG unit-based active harmonic damping method for grid-connected and islanding microgrid systems. An improved virtual impedance control method with a virtual damping resistor and a nonlinear virtual capacitor is proposed. The nonlinear virtual capacitor is used to compensate the harmonic voltage drop on the grid-side inductor of a DG unit *LCL* filter. The virtual resistor is mainly responsible for microgrid resonance damping. The effectiveness of the proposed damping method is examined using both a single DG unit and multiple parallel DG units.**

***Index Terms*—Active power filter, distributed power generation, droop control, grid-connected converter, microgrid, power quality, renewable energy system, resonance propagation, virtual impedance.**

I. Introduction

THE INCREASING application of nonlinear loads can led to significant harmonic pollution in a power distribution system. The harmonic distortion may excite complex resonances, especially in power systems with underground cables or subsea cables [22] and [23]. In fact, these cables with nontrivial parasite shunt capacitance can form an *LC* ladder network to amplify resonances. In order to mitigate system resonances, damping resistors or passive filters can be placed in the distribution networks [1]. Nevertheless, the mitigation of resonance propagation using passive components is subject to a few well-understood issues, such as power loss and additional investment. Moreover, a passive filter may even bring additional resonances if it is designed or installed without knowing detailed system configurations.

To avoid the adoption of passive damping equipment, various types of active damping methods have been developed. Among them, the resistive active power filter (R-APF) [2]–[8] is often considered as a promising way to realize better performance. Conventionally, the principle of R-APF is to emulate the behavior of passive damping resistors by applying a closed-loop current-controlled method (CCM) to power electronics converters. In this control category, the R-APF can be simply modeled as a virtual harmonic resistor if it is viewed at the distribution system level [2]. Additionally, a few modified R-APF concepts were also developed in the recent literature. In [6], the discrete tuning method was proposed to adjust damping resistances at different harmonic orders. Accordingly, the R-APF essentially works as a nonlinear resistor. In [5], the operation of multiple R-APFs was also considered, where an interesting droop control was designed to offer autonomous harmonic power sharing ability among parallel R-APFs.

On the other hand, renewable energy source (RES) based distributed generation (DG) units have been adopted to form flexible microgrids and their interfacing converters also have the opportunity to address different distribution system power quality issues [8], [9], [17]. For current-controlled DG units, the auxiliary R-APF function can be seamlessly incorporated into the primary DG real power injection function by modifying the current reference. However, conventional CCM can hardly provide direct voltage support during microgrid islanding operation. To overcome this limitation, an enhanced voltage-controlled method (VCM) [17] was recently proposed for DG units with high-order *LC* or *LCL* filters. It can be seen that the control method in [17] regulates the DG unit as virtual impedance, which is dependent on the existing feeder impedance. When the feeder impedance is inductive, this method could not provide enough damping effects to system resonance.

To achieve better operation of grid-connected and islanding microgrids, the paper considers a simple harmonic propagation model in which the microgrid is placed at the receiving end of the feeder. To mitigate the feeder harmonic distortions, a modified virtual impedance-based active damping method that consists of a virtual resistor and a virtual nonlinear capacitor is also proposed. The virtual capacitor eliminates the impacts of *LCL* filter grid-side inductor and the virtual resistor is interfaced to the receiving end of the feeder to provide active damping

Manuscript received September 5, 2013; revised March 19, 2014; accepted April 28, 2014. Date of publication July 15, 2014; date of current version February 16, 2015. The work was supported in part by the Natural Science and Engineering Research Council of Canada; in part by the Major International (Regional) Joint Research Project of the National Natural Science Foundation of China (NSFC) under Grant 61320106011; and in part by the Shandong Electric Power Research Institute, Shandong, China. Paper No. TEC-00521-2013.

J. He is with Accuenergy Canada Inc., Toronto, ON M2J 4P8, Canada (e-mail: hjinwei@ualberta.ca).

Y. W. Li is with the University of Alberta, Edmonton, AB T6G 2R3, Canada (e-mail: yunwei.li@ualberta.ca).

R. Wang is with the Shandong Electric Power Research Institute, State Grid Corporation of China, Beijing 100053, China (e-mail: 13698622826@163.com).

C. Zhang is with Shandong University, Jinan 250100, China (e-mail: zchui@sdu.edu.cn).

Color versions of one or more of the figures in this paper are available online at http://ieeexplore.ieee.org.

Digital Object Identifier 10.1109/TEC.2014.2332497

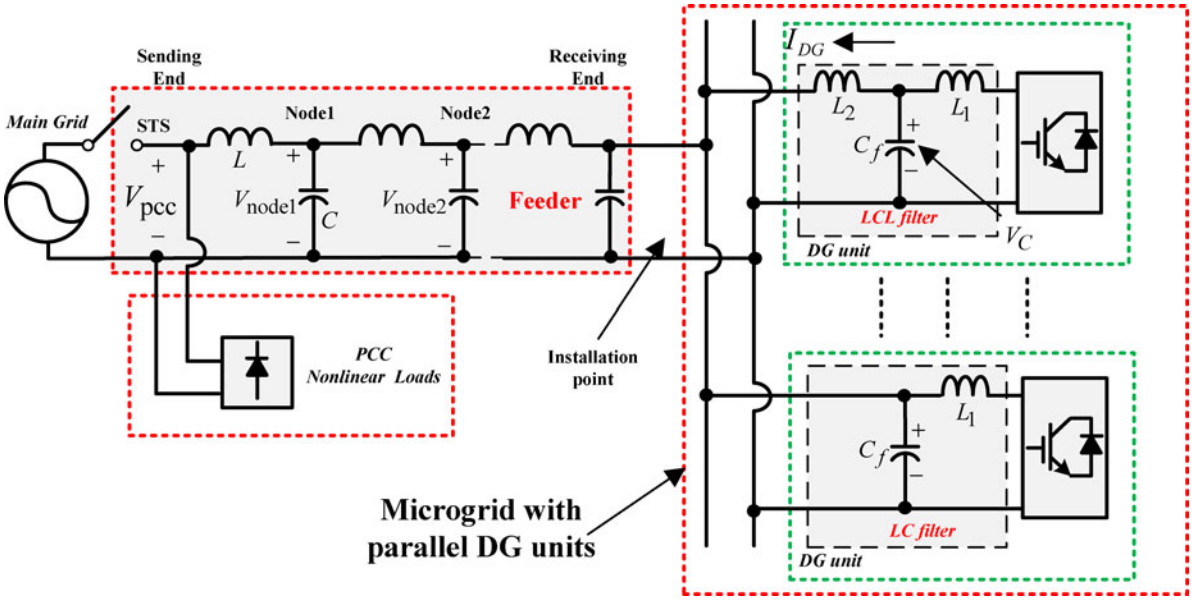

Fig. 1. Simplified one-line diagram of a single-phase microgrid.

service. Simulated results are provided to confirm the validity of the proposed method.

II. Modeling of DG Units in Microgrid System

Fig. 1 illustrates the configuration of a single-phase microgrid system, where a few DG units are interconnected to the point of common coupling (PCC) through a long underground feeder. For the sake of simplicity, this paper only adopts a simple microgrid configuration to demonstrate how the microgrid power quality is affected by resonance propagation. In addition, this paper also assumes that shunt capacitor banks and parasitic feeder capacitances are evenly distributed in the feeder [2], [3].

Note that the static transfer switch (STS) controls the operation mode of the microgrid. When the main grid is disconnected from the microgrid, the PCC nonlinear loads shall be supplied by the standalone DG units.

A. Distributed Parameter Model in Grid-Tied Operation

For a long feeder, as illustrated in Fig. 1, a lumped parameter model is not able to describe its resonance propagation characteristics. Alternatively, the distributed parameter model was discussed in [3] and [6], where the voltage distortions at PCC induce a harmonic voltage standing wave along the feeders. To make the discussion more straightforward, we assume that the microgrid in the feeder receiving end only consists of one DG interfacing converter. In the next section, the modeling of resonances in multiple DG-unit-based microgrid is discussed. With the aforementioned assumption, the equivalent circuit model of a grid-tied microgrid at the *k*th harmonic frequency is presented in Fig. 2, where the *k*th PCC harmonic voltage is assumed to be stiff and $V_{\mathrm{pcc}k}$. $V_k(x)$and $I_k(x)$ are the feeder *k*th harmonic voltage and harmonic current at position x. The length of the feeder is l.

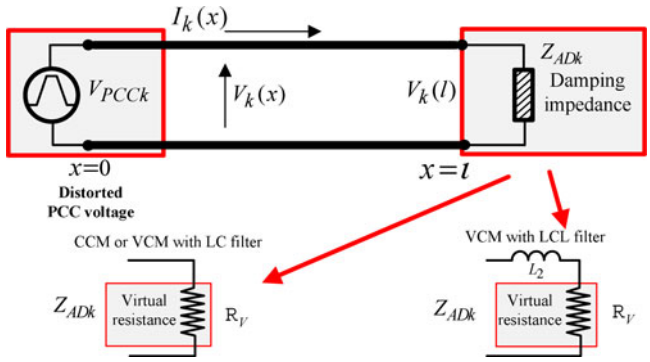

Fig. 2. Equivalent circuit of a single grid-connected DG unit at the *k*th harmonic frequency.

It is easy to obtain the harmonic voltage–current standing wave equations at the harmonic order *k* as

$$V_k(x) = Ae^{-\gamma x} + Be^{\gamma x} \tag{1}$$

$$I_k(x) = \frac{1}{z}(Ae^{-\gamma x} - Be^{\gamma x}) \tag{2}$$

where A and B are constants, which are determined by feeder boundary conditions. z and γ are the characteristics impedance [3] of the feeder without considering the line resistance as

$$z = \sqrt{\frac{L}{C}} \tag{3}$$

$$\gamma = jk\omega_f\sqrt{LC} \tag{4}$$

where ω_f is the fundamental angular frequency and L and C are the feeder equivalent inductance and shunt capacitance per kilometer, respectively.

1) DG Units with CCM and R-APF Control: To determine the boundary conditions of the feeder, the equivalent harmonic impedance ($Z_{\mathrm{AD}k}$) of the DG unit must be derived.

First, the current reference (I_{ref}) of a CCM-based DG unit can be obtained as

$$\begin{aligned} I_{\mathrm{ref}} &= I_{\mathrm{reff}} - I_{\mathrm{AD}} \\ &= I_{\mathrm{reff}} - \frac{H_D(s)\cdot V(l)}{R_V} \end{aligned} \tag{5}$$

where I_{reff} is the fundamental current reference for DG unit power control, I_{AD} is the harmonic current reference for system resonance compensation, $V(l)$ is the measured installation point voltage at the receiving end of the feeder, $H_D(s)$ is the transfer function of a harmonic detector, which extracts the harmonic components of the installation point voltage, and R_V is the command virtual resistance.

Without considering the delays in current tracking and harmonic detection, the DG unit works as a small resistor ($Z_{\mathrm{AD}k} = R_V$) at the selected harmonic order *k*. Note that for the conventional CCM-based DG unit without any system harmonic compensation, the current reference does not include any harmonic contents [corresponding to set R_V as ∞ in (5)]. Consequently, the conventional CCM-based DG unit can be simply modeled as an open-circuit connection at the receiving end.

2) DG Units with VCM and R-APF Control: In contrast to CCM-based methods, the VCM-based DG units indirectly regulate the power flow through the control of filter capacitor voltage V_C (see Fig. 1). For a conventional VCM-based DG unit without harmonic damping, the voltage magnitude and frequency reference [10] can be obtained from the droop control scheme as

$$\omega_{\mathrm{DG}} = \omega_f + D_P\cdot(P_{\mathrm{ref}} - P_{\mathrm{LPF}}) \tag{6}$$

$$E_{\mathrm{DG}} = E + D_q\cdot(Q_{\mathrm{ref}} - Q_{\mathrm{LPF}}) + \frac{K_Q}{s}(Q_{\mathrm{ref}} - Q_{\mathrm{LPF}}) \tag{7}$$

where ω_f and ω_{DG} are the nominal and reference angular frequencies. *E* and E_{DG} are the nominal and reference DG voltage magnitudes. P_{LPF} and Q_{LPF} are the measured power with low-pass filtering. D_p and D_q are the droop slopes of the controller. Note that with the integral control to regulate DG unit voltage magnitude in (7), the steady-state reactive power control error at the grid-tied operation is zero [10], [12]–[13]. Once the voltage magnitude reference and the frequency reference are determined, the ripple-free instantaneous voltage reference (V_{reff}) can be easily obtained.

The equivalent impedance of VCM-based DG unit with an *LC* filter has already been tuned to be resistive, by adding a DG line current (I_{DG}) feed-forward term to the voltage control reference [14]. Although previous VCM-based DG equivalent impedance shaping techniques mainly focus on improving the power sharing performance of multiple DG units in an islanding microgrid, similar idea can also be used to mitigate the harmonic propagation along the feeder as

$$\begin{aligned} V_{\mathrm{ref}} &= V_{\mathrm{reff}} - V_{\mathrm{AD}} \\ &= V_{\mathrm{reff}} - R_V\cdot(H_D(s)\cdot I_{\mathrm{DG}}) \end{aligned} \tag{8}$$

where V_{reff} is the fundamental voltage reference derived from droop control in (6) and (7), V_{AD} is the harmonic voltage reference for DG unit harmonic impedance shaping, I_{DG} is the measured DG unit line current (see Fig. 1), $H_D(s)$ is the transfer function of a harmonic detector, which extracts the harmonic components of DG unit line current, and R_V is the virtual resistance command.

Note that when a VCM-based DG unit with an *LC* filter is controlled without any harmonic impedance shaping target [by setting $R_V = 0$ in (8)], it essentially works as short-circuit connection ($Z_{\mathrm{AD}k} = 0$) at the harmonic frequencies.

Nevertheless, if an *LCL* filter is adopted as the DG output filter, the VCM-based control method using filter capacitor voltage regulation does not address the harmonic voltage drop on the grid-side inductor (L_2). Accordingly, the DG unit shall be modeled as the combination of a reactor and a resistor ($Z_{\mathrm{AD}k} = R_V + jk\omega_f L_2$) when (8) is applied to the DG unit (see Fig. 2). As will be discussed later, the imaginary part of $Z_{\mathrm{AD}k}$ may affect the voltage harmonic suppression performance of the system.

Since a grid-connected DG unit using either CCM or VCM can be modeled by an equivalent harmonic impedance at the receiving end of the feeder, the following boundary conditions can be obtained:

$$\frac{V_k(\ell)}{I_k(\ell)} = Z_{\mathrm{AD}k} \tag{9}$$

$$V_k(0) = V_{\mathrm{PCC}k}. \tag{10}$$

By solving (1), (2), (9), and (10), the harmonic voltage propagation at the harmonic order *k* can be expressed as

$$V(x)_k = \frac{Z_{\mathrm{AD}k}\cosh(\gamma(l-x)) + z\sinh(\gamma(l-x))}{Z_{\mathrm{AD}k}\cosh(\gamma l) + z\sinh(\gamma l)} V_{\mathrm{PCC}k}. \tag{11}$$

With the obtained equation in (11), the impact of DG active damping scheme to the harmonic voltage propagation along the feeder can be easily analyzed.

Note that when the microgrid feeder is purely *RL* impedance, the DG unit can still work as a virtual harmonic resistor at the end of the feeder. In this case, the DG unit has the capability of absorbing some PCC nonlinear load current if it is designed and controlled properly [9] and [20].

B. Distributed Parameter Model in Islanding Operation

The previous section focuses on the analysis of grid-tied DG units. For an islanding microgrid system, the VCM operation of DG units is needed for direct voltage support. To the best of the authors' knowledge, the quantitative analysis of islanding microgrid harmonic propagation is not available.

When only a single DG unit is placed in the islanding system, constant voltage magnitude and constant frequency (CVMCF) control can be used. On the other hand, for the operation of multiple DG units in the microgrid (see Fig. 1), the droop control method in (6) and (7) [by setting $K_Q = 0$ in (7)] shall be employed to realize proper power sharing among these DG units. Considering the focus of this section is to investigate the

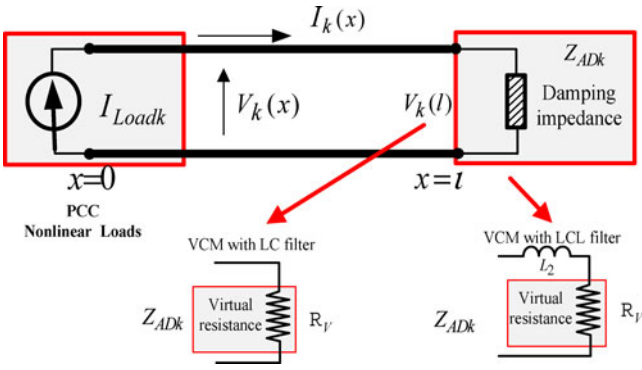

Fig. 3. Equivalent circuit of a single islanding DG unit at the *k*th harmonic frequency.

harmonic voltage damping in a stand-alone islanding system, a single DG unit at the receiving end of the feeder is considered.

The circuit model of an islanding system at the harmonic order *k* is illustrated in Fig. 3, where VCM-based DG unit is also modeled as an equivalent harmonic impedance using the control scheme in (8). The nonlinear PCC load in this case is modeled as a harmonic current source at the sending end of the feeder [3].

With the knowledge of boundary conditions at both sending and receiving ends as

$$I_k(0) = I_{\mathrm{Load}k} \tag{12}$$

$$\frac{V_k(\ell)}{I_k(\ell)} = Z_{\mathrm{AD}k} \tag{13}$$

the *k*th harmonic voltage distortion along the feeder can be obtained

$$V_k(x) = \left(\frac{e^{-\gamma x}}{1 + ((z - Z_{\mathrm{AD}k})/(z + Z_{\mathrm{AD}k}))e^{-2\gamma \ell}} - \frac{e^{\gamma x}}{1 + (z + Z_{\mathrm{AD}k})/(z - Z_{\mathrm{AD}k})e^{2\gamma \ell}} \right) z I_{\mathrm{Load}k} \tag{14}$$

From (14), it can be noticed that the voltage propagation in an islanding system harmonic is also related to the DG-unit-equivalent harmonic impedance. In order to maintain satisfied voltage quality, the equivalent harmonic impedance of islanding DG units shall also be properly designed.

III. Evaluation of Damping Performance

In this section, the performance of VCM-based DG units at different operation modes is investigated.

A. Evaluation of a Single DG Unit at the End of the Feeder

1) Grid-Tied Operation: First, the performance of a grid-tied DG unit with an *LCL* filter is investigated. The system parameters are listed in Table I. Fig. 4 shows harmonic voltage distortions along a 6 km feeder. The harmonic voltage distortion factor here is normalized to the voltage distortions at PCC as $V(x)_k/V_{\mathrm{PCC}k}$. When the conventional VCM without damping is applied to the DG unit, the *LCL* filter capacitor voltage is ripple free and the DG unit works as an inductor (L_2) at the harmonic frequencies. It can be seen that the feeder is sensitive to 7th harmonic voltage distortion at the PCC. When the DG unit is controlled by the modified voltage control reference as shown in (8), it works as an equivalent *RL* impedance at the

TABLE I
Feeder Parameters

System Parameter	Value
Feeder length	6 km
Number of nodes	7
Line inductance *L*	1 mH/km
Capacitance *C*	20 μF/km
DG unit parameter	Value
With *LCL* filter	$L_1 = 2\mathrm{mH}\ L_2 = 3.5\ m\mathrm{H}\ C_f = 20\mu F$
Command virtual resistance	$RV = 5.5\ \omega$

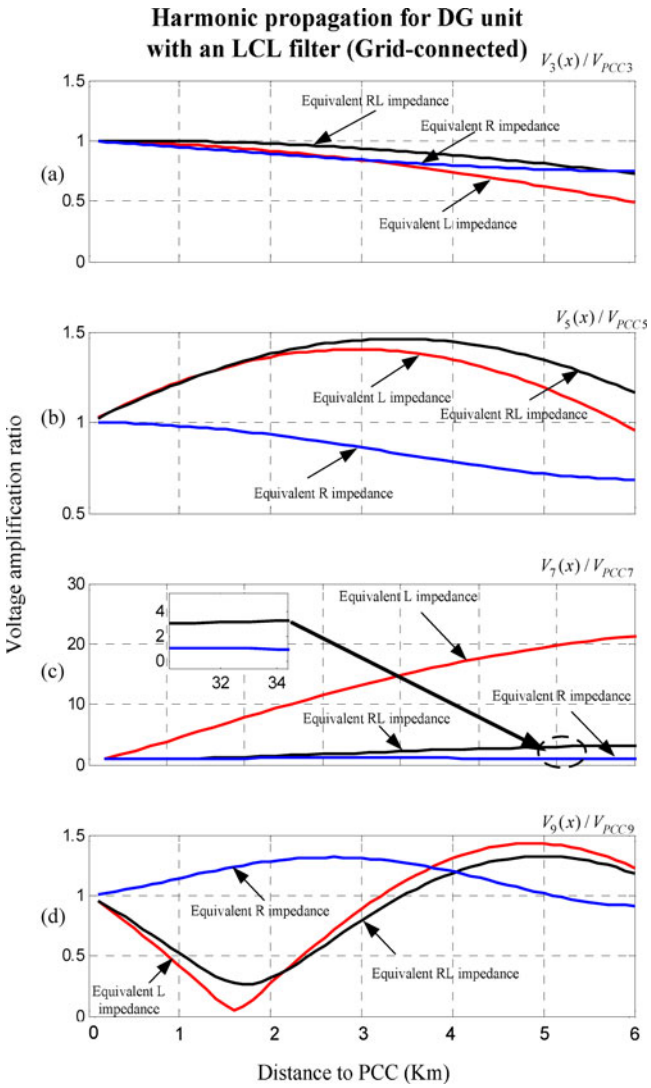

Fig. 4. Harmonic voltage amplification in a single DG unit grid-connected operation [(a)–(d): amplification ratio at 3rd, 5th, 7th, and 9th harmonic frequencies].

receiving end of the feeder. Accordingly, the most obvious 7th harmonic voltage propagation is effectively reduced as shown in Fig. 4(c).

When a DG unit is coupled to the distribution system with an *LC* filter, the DG unit is equivalent to a harmonic damping resistor by the control scheme in (8). The corresponding performance of the system at different harmonic orders is also investigated in Fig. 4. When a virtual harmonic damping resistor is placed at the end of the feeder, the voltage distortions at different positions of the feeder can be closer to the harmonic voltage content at PCC. Note that for a CCM-based DG unit using the harmonic compensation scheme in (5), the DG unit is also equivalent to a harmonic resistor at the harmonic frequencies. Therefore, the obtained waveforms can be used to evaluate the performance of CCM-based DG units in a similar way.

2) Stand-alone Operation: In addition, a DG unit with an *LCL* filter in a standalone islanding system is also examined. In contrast to the performance during grid-tied operation, the voltage distortion at PCC is not stiff in this case and it is dependent on the harmonic current from the PCC nonlinear loads. As a result, the harmonic voltage amplification factor $V(x)_k/V_{\mathrm{PCC}k}$ that is used in grid-tied systems is not very appropriate for an islanded system. Alternatively, the feeder harmonic voltage over PCC load harmonic current $(V_k(x)/V_{\mathrm{Load}k})$ can be used to describe the harmonic propagation characteristic of the system. The associated harmonic propagation performance is obtained in Fig. 5. As illustrated in Fig. 5(a), the 3rd harmonic current of PCC loads induces nontrivial harmonic voltage distortions at PCC when conventional VCM-controlled DG unit without using active damping is applied. On the other hand, the active damping using *RL* harmonic impedance [corresponding to the DG unit with an *LCL* filter controlled by (8)] can effectively reduce the 3rd harmonic voltage distortion. Moreover, when only a damping resistor is placed at the end of feeder, the 3rd harmonic voltage distortion is further reduced.

In addition to the performance at 3rd harmonic frequency, both equivalent *R* and equivalent *RL* impedances can effectively suppress the long feeder voltage distortions at 5th, 7th, and 9th harmonic frequencies. Note that when *R* impedance is used, the amplitude of harmonic voltage distortions along the feeder is closer to that at PCC.

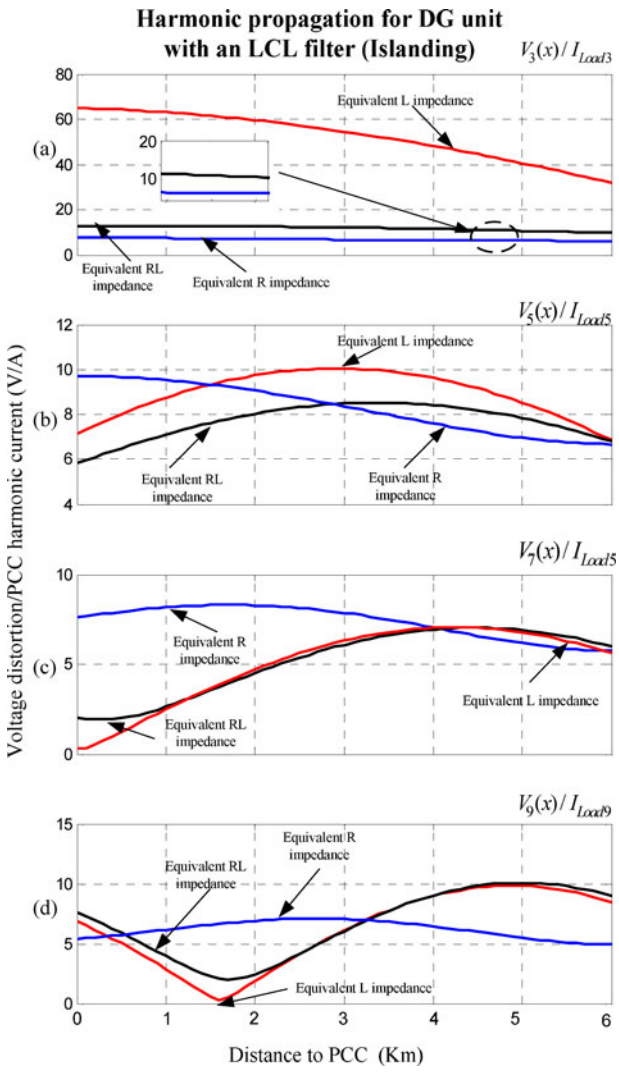

Fig. 5. Harmonic voltage amplification in a single DG unit islanding operation [(a)–(d): amplification ratio at 3rd, 5th, 7th, and 9th harmonic frequencies].

B. Evaluation of Multiple DG Units at the End of the Feeder

The performance of a microgrid with multiple DG units is increasingly discussed in the recent literature [12]–[16]. In addition to achieve proper power sharing among multiple DG units, realizing superior harmonic damping performance in a collaborative manner is also attractive [17]. For parallel DG units as shown in Fig. 1, they shall share the active damping current according to their respective power rating [4].

However, phase angle difference between damping resistor [corresponding to VCM-based DG unit with an *LC* filter controlled by (8)] and *RL* damping impedance [corresponding to VCM-based DG unit with an *LCL* filter controlled by (8)] may bring some harmonic circulating currents.

To simplify the discussion, two VCM controlled DG units at the same power rating are used to equally share the harmonic current associated with the active damping control. If the DG unit with an *LC* filter is controlled as a harmonic damping resistor *R* while the other one with an *LCL* filter is regulated as the *RL* damping impedance, the corresponding circuit diagram at the harmonic order *k* can be illustrated in Fig. 6. As shown, the harmonic impedances of these two DG units have the same resistive part. However, for the DG unit with an *LCL* filter, its equivalent impedance also has an inductive part $jk\omega_f L_2$.

The circulating current at *k*th harmonic order can also be observed from the phasor diagram in Fig. 7. As demonstrated, the harmonic damping current of DG unit 1 is in-phase with the harmonic voltage at the receiving end of the feeder. At the same time, the current of DG unit 2 is lagging of the harmonic voltage $V_k(l)$. With unequal current phase angles, harmonic circulating current among DG units is introduced.

Note that to estimate the active damping current of each DG unit, the knowledge of voltage distortion $V_k(l)$ at the receiving

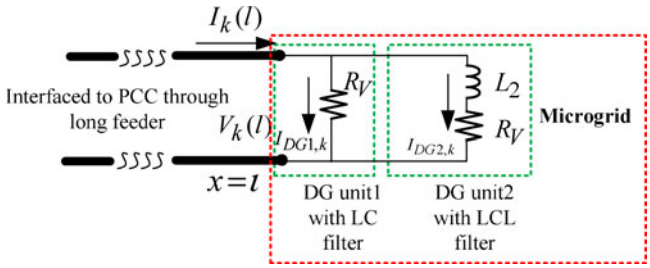

Fig. 6. Circuit diagram of a double-DG-based microgrid at the *k*th harmonic frequency.

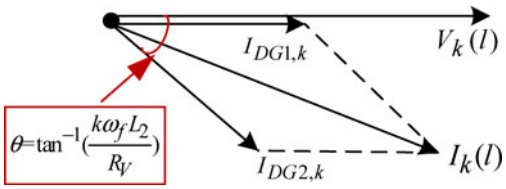

Fig. 7. Phasor diagram of the harmonic circulating current among parallel DG units.

end of the feeder is needed. In this case, microgrid equivalent harmonic impedance $Z_{\mathrm{AD}k,\mathrm{microgrid}}$ shall be used to replace a single DG unit equivalent harmonic impedance $Z_{\mathrm{AD}k}$ in (11) and (14). For a microgrid with two DG units, as shown in Fig. 6, its equivalent impedance is the parallel equivalent impedance of parallel DG units as

$$Z_{\mathrm{AD}k,\mathrm{microgrid}} = \frac{Z_{\mathrm{AD}k,\mathrm{DG1}} \cdot Z_{\mathrm{AD}k,\mathrm{DG2}}}{Z_{\mathrm{AD}k,\mathrm{DG1}} + Z_{\mathrm{AD}k,\mathrm{DG2}}} = \frac{(R_V + jk\omega_f L_2) \cdot R_V}{2R_V + jk\omega_f L_2}. \quad (15)$$

IV. Realization of Virtual Damping Impedance Through DG Voltage Control

It has been clarified that an *LCL* filter grid-side inductor (L_2) can affect the performance of distribution system harmonic suppression, especially in the case of multiple DG units. In order to compensate the impact of *LCL* filter grid-side inductor, the harmonic voltage damping scheme as shown in (8) shall be further improved.

A. Conventional Voltage Tracking

First, a negative virtual inductor can be produced by VCM. Accordingly, the modified voltage reference is obtained as

$$V_{\mathrm{ref}} = V_{\mathrm{reff}} - V_{\mathrm{AD}} - V_{\mathrm{Comp}} = V_{\mathrm{reff}} - R_V \cdot H_D(s) \cdot I_{\mathrm{DG}} - s(-L_2) \cdot H_D(s) \cdot I_{\mathrm{DG}}. \quad (16)$$

Comparing (16) to (8), it can be noticed that an additional voltage compensation term V_{Comp} is deducted from the voltage control reference. The aim of this voltage compensation term is to cancel the harmonic voltage drop on the grid-side *LCL* filter inductor L_2.

Once the modified voltage reference in (16) is determined, a high bandwidth voltage controller, such as deadbeat control, *H*-infinity control, and multiple loop control, can be selected to ensure satisfied *LCL* filter capacitor voltage (V_C) tracking.

By further looking into (16), one can find that the implementation of virtual inductor involves derivative operation, which may adversely amplify system background noises. For instance, if a band-stop filter is selected to filter out the fundamental components as

$$H_D(s) = 1 - \frac{2\omega_{\mathrm{BP}} s}{s^2 + 2\omega_{\mathrm{BP}} s + \omega_f^2} \quad (17)$$

where ω_{BP} is the cutoff bandwidth of the band-stop filter, the voltage compensation term V_{Comp} in (16) can be expressed as

$$V_{\mathrm{Comp}} = s(-L_2) \cdot H_D(s) I_{\mathrm{DG}} = \left(-sL_2 + \frac{2\omega_{\mathrm{BP}} L_2 s^2}{s^2 + 2\omega_{\mathrm{BP}} s + \omega_f^2} \right) \cdot I_{\mathrm{DG}}. \quad (18)$$

The diagram of a DG unit with negative virtual inductor control is shown in Fig. 8. As illustrated, the DG unit is interfaced to long feeder with an *LCL* filter. First, the real power frequency droop control (6) and the reactive power voltage magnitude droop control (7) in the power control loop [10], [18] and [19] are used to determine the fundamental voltage reference V_{reff} Note that this droop control method can also realize proper fundamental power sharing between multiple islanding DG units, without using any communications between them [10]. V_{Comp} in (18) is deducted from the reference voltage V_{reff}. In order to alleviative the impact of derivative operator in V_{Comp}, a high-pass filter can be used as an approximation [14]. However, as already been pointed out in [12] and [13], the adoption of high-pass filter introduces some magnitude and phase errors, which can degrade the performance of the compensation term V_{Comp}.

B. Implementation of Nonlinear Virtual Capacitor

In this subsection, a well-understood double-loop voltage controller is selected for DG unit voltage tracking. In the outer filter capacitor voltage control loop, the proportional and multiple resonant (PR) controllers are used as

$$I_{\mathrm{Inner}} = G_{\mathrm{Outer}}(s) \cdot (V_{\mathrm{ref}} - V_C) = \left(K_P + \sum_k \frac{2K_{ik}\omega_{ck} s}{s^2 + 2\omega_{ck} s + (k\omega_f)^2} \right) \cdot (V_{\mathrm{ref}} - V_C) \quad (19)$$

where K_P is the outer loop proportional gain, K_{ik} is the gain of resonant controller at fundamental and selected harmonic frequencies, ω_{ck} is the cutoff bandwidth, and I_{Inner} is the control reference for the inner control loop.

In the inner loop controller ($G_{\mathrm{Inner}}(s)$), a simple proportional controller (K_{inner}) is employed and the inverter output current (I_{inv}) is measured as the feedback.

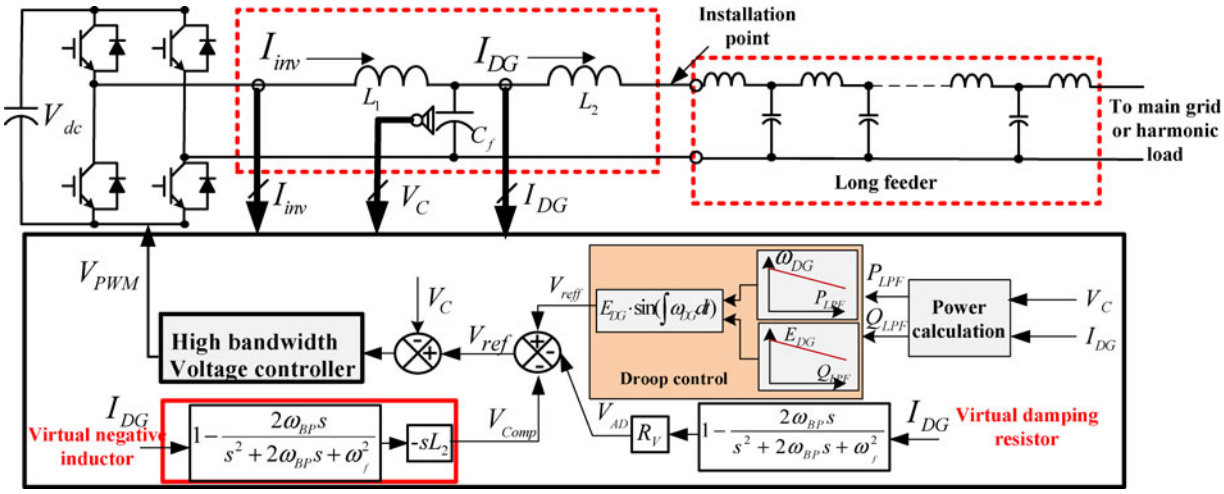

Fig. 8. Mitigation of distribution feeder harmonic propagation using virtual resistor and virtual negative inductor.

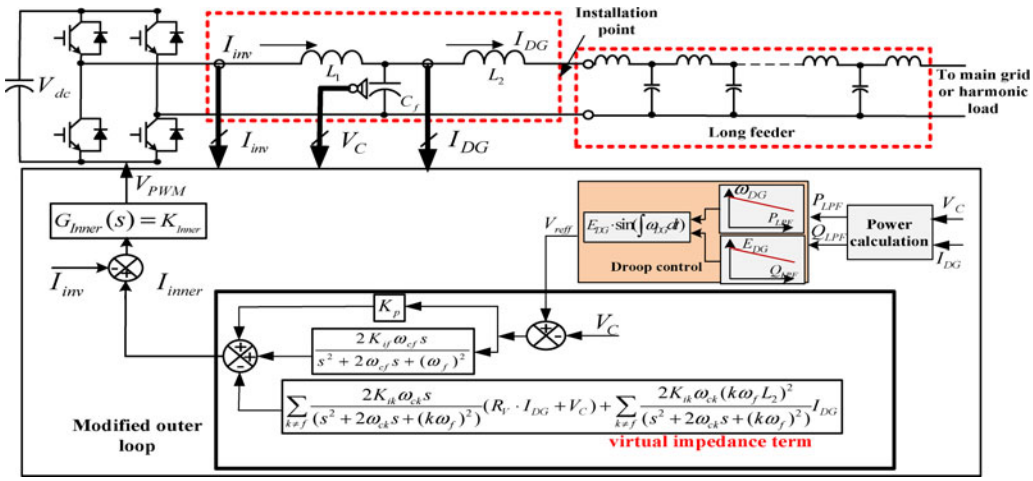

Fig. 9. Mitigation of harmonic propagation using virtual resistor and nonlinear virtual capacitor.

By further utilizing the resonant controllers in (19) to avoid the derivative operation, the paper proposes a nonlinear virtual capacitor control method instead of the use of negative virtual inductor. This is because the impedance of a capacitor also has 90° lagging phase angle, which is the same as that in a negative inductor. However, for a capacitor with fix capacitance, its impedance magnitude is in inverse proportion to harmonic orders. This feature is in contrast to the characteristics of a virtual inductor. To cancel the impacts of *LCL* filter grid-side inductor without using derivative operation, a nonlinear virtual capacitor with the following frequency-dependent capacitance is needed:

$$L_2(\omega_f t) - \frac{1}{C_{Vk}(\omega_f t)} = 0 \tag{20}$$

where ω_f is the fundamental angular frequency and C_{Vt} is the command capacitance at the harmonic order *t*.

Note that an *LCL* filter inductance often has some attenuation, if the line current is higher than the current rating of the filter chokes. In this case, an online estimation method [21] can be used to identify the real-time inductance of the *LCL* filter and the virtual capacitance in (20) shall be modified accordingly.

With the control of nonlinear virtual capacitor as shown in (20), the harmonic impact of the inductor L_2 could be properly compensated. To realize this task, the traditional harmonic detector in (17) can be replaced by a family of selective harmonic separators to extract DG line current harmonic contain ($I_{\mathrm{DG}t}$) at each selected harmonic frequency. Afterwards, the voltage drops on the nonlinear virtual capacitor can be obtained as

$$V_{\mathrm{Comp}} = \sum_t \frac{1}{sC_{Vt}} \cdot I_{\mathrm{DG}t} = \sum_t \frac{1}{sC_{Vt}} \cdot (H_{Dt}(s) \cdot I_{\mathrm{DG}}) \tag{21}$$

where $H_{Dt}(s)$ is the harmonic detector to detect the *t*th DG harmonic current $I_{\mathrm{DG}t}$.

It can also be seen that parallel resonant controllers used in the outer loop voltage control in (19) are essentially a set of band-pass filters with narrow bandwidth ω_{ck} and amplified magnitudes K_{ik}. Indeed, the harmonic selective capability has already been embedded in the resonant controllers. If arranged

TABLE II
DG UNIT PARAMETERS

Control Parameter	Value
Rated voltage	RMS 60 V
Rated frequency	$f = 60$ Hz
Droop coefficients	$D_p = 1/300$; $D_p = 1/300$; $K_Q = 1/30$;
Proportional gain	$Kp1 = 0.11$
Resonant gain	$Kif = 20$, $Ki3 = 15$, $Ki5 = 15$, $Ki7 = 15$, $Ki9 = 10$
Cutoff frequency	$\omega_{ck} = 4$ rad/s ($K = f$, 3, 5, 7, and 9)
Inner loop controller	$K_{\text{inner}} = 20$
DC link voltage	$V_{\text{dc}=240V}$
Sampling and switching frequency	12 kHz
Circuit parameter	Value
LCL filter	$L_1 = 2$ mH $L_2 = 3.5$ mH $C_f = 20$ μF
LC filter	$L_1 = 2$ mH $L_2 = 0$ mH $C_f = 20$ μF (DG unit 1 in Figs. 14 and 15)
Command virtual resistance	$R_V = 5.5$ ω (DG unit in Figs. 10–13) $R_V = 11$ ω (DG unit 1 and DG unit 2 in Figs. 14 and 15)

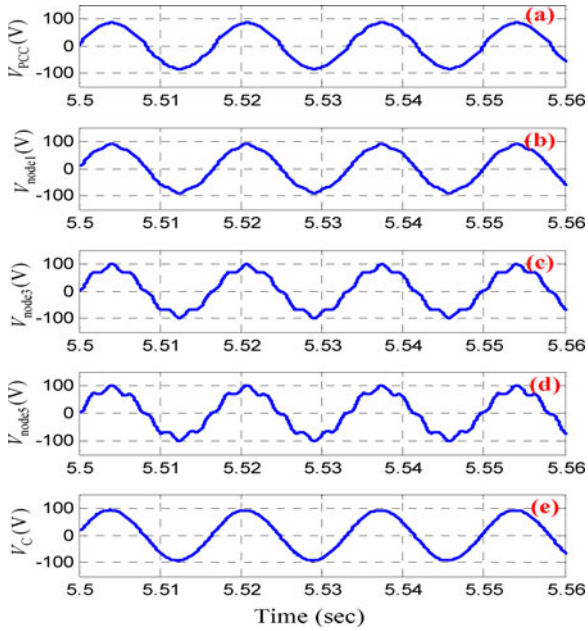

Fig. 10. Harmonic voltage amplification during a single DG unit grid-connected operation (without damping) [from upper to lower: (a) PCC voltage (THD = 4.0%); (b) node 1 voltage (THD = 4.56%); (c) node 3 voltage (THD = 10.91%); (d) node 5 voltage (THD = 12.59%); (e) DG unit filter capacitor voltage (THD = 0.38%)].

properly, resonant controllers can be further utilized to realize the control of virtual nonlinear capacitor.

First, the instantaneous DG voltage reference V_{reff} derived from (6) and (7) is always ripple-free [17] and the fundamental resonant controller can be adopted for V_{reff} tracking. In addition, the regulation of virtual resistor and virtual capacitor mainly focuses on the performance at selected harmonic frequencies. Therefore, parallel harmonic resonant controllers can be utilized to control these virtual impedances. Once the conventional PR controller is separated into two parts, the modified outer loop control scheme is illustrated as follows:

$$I_{\text{Inner}} = \left(K_{P1} + \frac{2K_{if}\omega_{cf}s}{s^2 + 2\omega_{cf}s + (\omega_f)^2}\right) \cdot (V_{\text{reff}} - V_C) + \sum_{k\neq f} \frac{2K_{ik}\omega_{ck}s}{(s^2 + 2\omega_{ck}s + (k\omega_f)^2)}(-V_{\text{AD}} - V_{\text{comp}} - V_C). \quad (22)$$

Combining (20), (21), and (22) yields

$$I_{\text{Inner}} = \left(K_{P1} + \frac{2K_{if}\omega_{cf}s}{s^2 + 2\omega_{cf}s + (\omega_f)^2}\right) \cdot (V_{\text{reff}} - V_C) - \sum_{t\neq f} \frac{2K_{ik}\omega_{ck}s}{(s^2 + 2\omega_{ck}s + (t\omega_f)^2)}(R_V \cdot H_D(s) \cdot I_{\text{DG}} + V_C) - \left[\sum_{t\neq f} \frac{2K_{ik}\omega_{ck}s}{(s^2 + 2\omega_{ck}s + (t\omega_f)^2)} \cdot \left(\sum_{t\neq f} \frac{(t\omega_f L_2)^2}{s} H_{Dt}(s) \cdot I_{\text{DG}}\right)\right]. \quad (23)$$

Note that the $H_D(s)$ is a harmonic detector, which has 0 db and 0° response at all selected harmonic frequencies and $H_{Dt}(s)$ is a selective harmonic detector which only has 0 db and 0° response at the *t*th harmonic frequency. By further utilizing the harmonic selective feature of harmonic resonant controllers in the PR controller, (23) can be further simplified as

$$I_{\text{Inner}} = \left(K_{P1} + \frac{2K_{if}\omega_{cf}s}{s^2 + 2\omega_{cf}s + (\omega_f)^2}\right) \cdot (V_{\text{reff}} - V_C) - \sum_{k\neq f} \frac{2K_{ik}\omega_{ck}s}{(s^2 + 2\omega_{ck}s + (k\omega_f)^2)}(R_V \cdot I_{\text{DG}} + V_C) - \sum_{k\neq f} \frac{2K_{ik}\omega_{ck}(k\omega_f L_2)^2}{(s^2 + 2\omega_{ck}s + (k\omega_f)^2)} I_{\text{DG}}. \quad (24)$$

With this modified outer loop controller, the DG unit fundamental voltage tracking and harmonic virtual impedance regulation can be realized separately. The detailed DG controller with the control of virtual nonlinear capacitor is shown in Fig. 9. In the revised controller, the harmonic voltage references associated with virtual resistor and virtual capacitor are only regulated by the harmonic resonant controllers. It can be seen that the derivative operator in Fig. 8 is avoided in Fig. 9.

It is true that the small proportional gain K_{P1} in (24) still induces some interference between fundamental and harmonic components regulation. However, the proportional gain in the PR controller is normally very small compared to resonant gains. In this paper, a small proportional gain ($K_{P1} = 0.11$) is

TABLE III
HARMONIC SPECTRUM OF A GRID-CONNECTED MICROGRID WITHOUT ACTIVE DAMPING (CORRESPONDING TO FIG. 10)

	3rd harmonic	5th harmonic	7th harmonic	9th harmonic	11th harmonic	13th harmonic	THD
PCC voltage	2.00%	2.00%	2.00%	2.00%	0%	0%	4.00%
Node 1 voltage	1.91%	2.41%	2.89%	1.31%	0.05%	0.03%	4.56%
Node 3 voltage	1.65%	2.92%	10.37%	0.74%	0.03%	0.04%	10.91%
Node 5 voltage	1.24%	2.57%	12.31%	2.07%	0.01%	0.02%	12.59%
DG voltage	0.02%	0.04%	0.10%	0.14%	0.15%	0.2%	0.38%

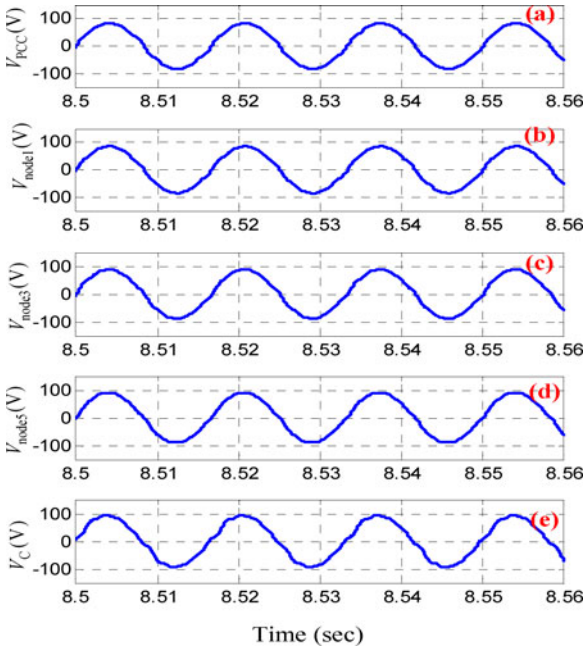

Fig. 11. Harmonic voltage amplification during a single DG unit grid-connected operation (with virtual nonlinear capacitor and resistor based active damping) [from upper to lower: (a) PCC voltage (THD = 4.0%); (b) node 1 voltage (THD = 4.1%); (c) node 3 voltage (THD = 3.7%); (d) node 5 voltage (THD = 3.2%); and (e) DG unit filter capacitor voltage (THD = 5.4%)].

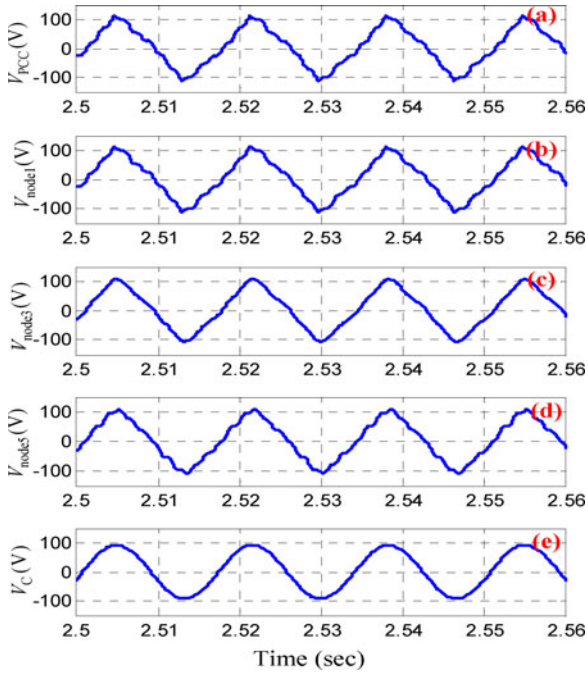

Fig. 12. Harmonic voltage amplification during a single DG unit islanding operation (without damping) [from upper to lower: (a) PCC voltage (THD = 15.2%); (b) node 1 voltage (THD = 14.7%); (c) node 3 voltage (THD = 11.9%); (d) node 5 voltage (THD = 10.5%); and (e) DG unit filter capacitor voltage (THD = 1.6%)].

selected to ensure that there is no noticeable coupling between the fundamental and the harmonic DG voltage tracking. With aforementioned efforts, the derivative operation is successfully avoided by using the proposed virtual nonlinear capacitor.

V. VERIFICATION RESULTS

Simulated results have been obtained from a single-phase low voltage microgrid. To emulate the behavior of six kilometers feeder with distributed parameters, a DG unit with an *LCL* filter is connected to PCC through a ladder network with six identical *LC* filter units (see Fig. 1). Each *LC* filter represents 1 km feeder. The parameters of these *LC* filters are selected to be the same as these in Table I. To provide some passive damping effects to the feeder, the *LC* filter inductor stray resistance is set to 0.12 Ω. The detailed DG unit control parameters are listed in Table II.

A. Single DG Unit Grid-Tied Operation

At first, the performance of a grid-connected DG unit with an *LCL* filter is examined. The PCC voltage in this simulation is stiff and it has 2.0% distortion at each lower order harmonic frequency (3rd, 5th, 7th, and 9th harmonics). Consequently, the total harmonic distortion (THD) of PCC voltage is 4.0%. When the conventional VCM method without damping is applied to the DG unit, the harmonic voltages at PCC, nodes 1, 3, 5, and DG unit filter capacitor are presented in Fig. 10. The node numbers here represent the distance (in kilometers) from the voltage measurement point to PCC. The harmonic spectrum of node voltages (corresponding to Fig. 10) is provided from upper to lower in Table III. It can be seen the 7th harmonic voltage is more obviously amplified at the nodes 3 and 5. This is consistent with the analysis in Fig. 4(c), where the feeder is sensitive to the 7th harmonic voltage at PCC. At the same time, the DG unit *LCL* filter capacitor voltage is almost ripple-free as shown in channel (e), as no damping control scheme is applied to the DG unit.

When the proposed control method with a virtual nonlinear capacitor and a virtual damping resistor as illustrated in Fig. 9 is applied to the DG unit, the harmonic voltage drops on the

TABLE IV
HARMONIC SPECTRUM OF AN ISLANDING MICROGRID WITHOUT ACTIVE DAMPING (CORRESPONDING TO FIG. 12)

	3rd harmonic	5th harmonic	7th harmonic	9th harmonic	11th harmonic	13th harmonic	THD
PCC voltage	13.19%	2.95%	0.29%	1.66%	6.58%	0.54%	15.19%
Node 1 voltage	11.96%	3.68%	0.39%	1.07%	6.62%	1.06%	14.67%
Node 3 voltage	10.05%	4.35%	1.45%	0.66%	1.09%	0.61%	11.93%
Node 5 voltage	7.54%	3.83%	1.73%	1.76%	5.98%	0.86%	10.51%
DG voltage	0.10%	0.05%	0.02%	0.45%	1.43%	0.2%	1.60%

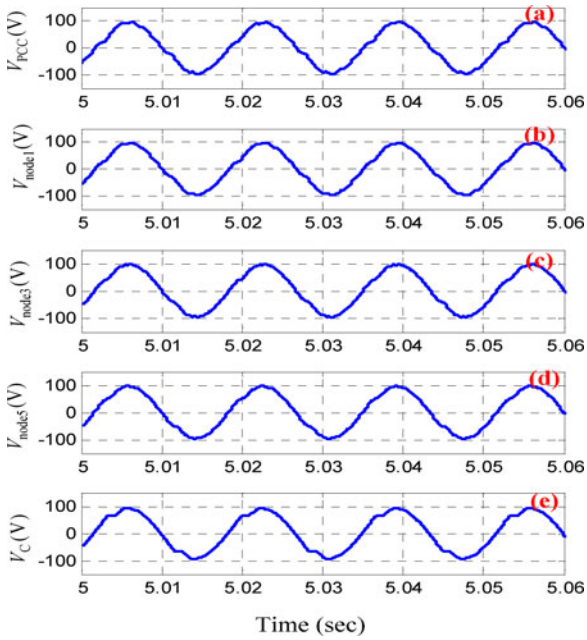

Fig. 13. Harmonic voltage amplification during a single DG unit islanding operation (with virtual nonlinear capacitor and resistor based active damping) [from upper to lower: (a) PCC voltage (THD $= 6.1\%$); (b) node 1 voltage (THD $= 6.0\%$); (c) node 3 voltage (THD $= 5.2\%$); (d) node 5 voltage (THD $= 5.3\%$); and (e) DG unit filter capacitor voltage (THD $= 7.1\%$)].

LCL filter grid-side inductor (L_2) are compensated and the DG unit behaves as a damping resistor at the end of the feeder. The results in Fig. 11 show that the resonance along the feeder is mitigated. However, compared to the situation without any damping in Fig. 10(e), the capacitor voltage of the DG unit as shown in Fig. 11(e) is distorted due to the regulation of virtual harmonic impedance.

B. Single DG Unit Islanding Operation

In addition to grid-connected operation, the performance of a single DG unit in islanding operation is also investigated. In this case, the PCC load is a single-phase diode rectifier and it is supplied by the DG unit through long feeder.

When the conventional VCM without damping is adopted, the performance of the system is obtained in Fig. 12. Similar to the grid-tied operation, the voltage waveforms at PCC, nodes 1, 3, and 5, and DG unit filter capacitor are shown from channels (a) to (e), respectively. To investigate the detailed performance of the system in this case, harmonic spectrum of node voltages is provided in Table IV. It can be easily seen that the third voltage distortions are more obviously amplified. This performance is also consistent with the theoretical analysis in Fig. 5.

When the virtual impedance control, as shown in Fig. 9, is used in the DG unit, the enhanced performance is shown in Fig. 13. It demonstrates that the third harmonic distortion observed in Fig. 12 is effectively suppressed.

C. Multiple DG Units Grid-Tied Operation

To verify the circulating harmonic current between multiple DG units, two grid-connected DG units at the same power rating are placed at the receiving end of the feeder. In this simulation, DG unit 1 is interfaced to the feeder receiving end with an *LC* filter while DG unit 2 has an *LCL* filter. The PCC voltage harmonics are selected to be the same as that in Fig. 10.

When both DG units are operating without any virtual impedance control, DG unit 1 essentially behaves as short circuit at the harmonics and DG unit 2 works as an equivalent inductor L_2, The voltage waveform along the feeder is shown in the first column of Fig. 14. In this case, there are some voltage distortions at the nodes 1 and 3. When only virtual resistor regulation using (8) is applied to both DG units, it can be seen from the second column of Fig. 14 that harmonic voltage distortions are mitigated. Finally, DG unit 2 is further controlled with a nonlinear virtual capacitor to compensate the effects of its *LCL* filter grid-side inductor, the associated voltage waveform is shown in the third column of Fig. 14.

Although the difference between the second and third columns of Fig. 14 is not very obvious, the harmonic circulating current between parallel DG units can be noticeable. When both of the DG units are controlled by (8), the system appears some harmonic circulating currents as shown in the first column of Fig. 15. These results agree with the discussion in Figs. 6 and 7. Moreover, when the nonlinear virtual capacitor control is also applied to DG unit 2, the harmonic voltage drop on its *LCL* filter grid-side inductor can be compensated and it also behaves as a virtual harmonic resistor. As a result, the harmonic circulating current among parallel DG units is effectively reduced. The improved harmonic current sharing performance is shown in the second column of Fig. 15.

VI. CONCLUSION

In this paper, a microgrid resonance propagation model is investigated. To actively mitigate the resonance using DG units, an enhanced DG unit control scheme that uses the concept of virtual impedance is proposed. Specifically, the capacitive

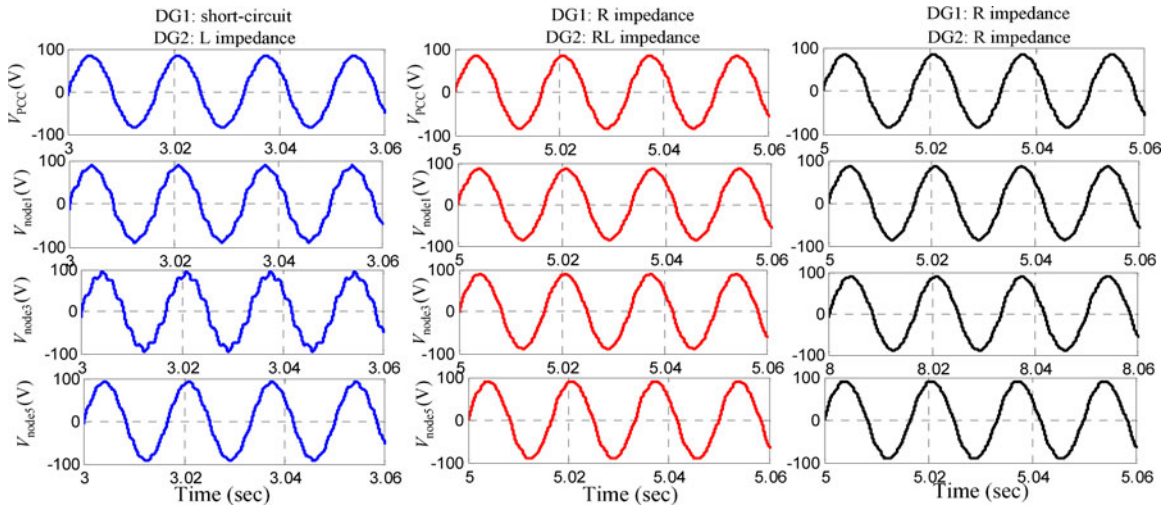

Fig. 14. Harmonic voltage amplification along the feeders (grid-tied operation of two parallel DG units).

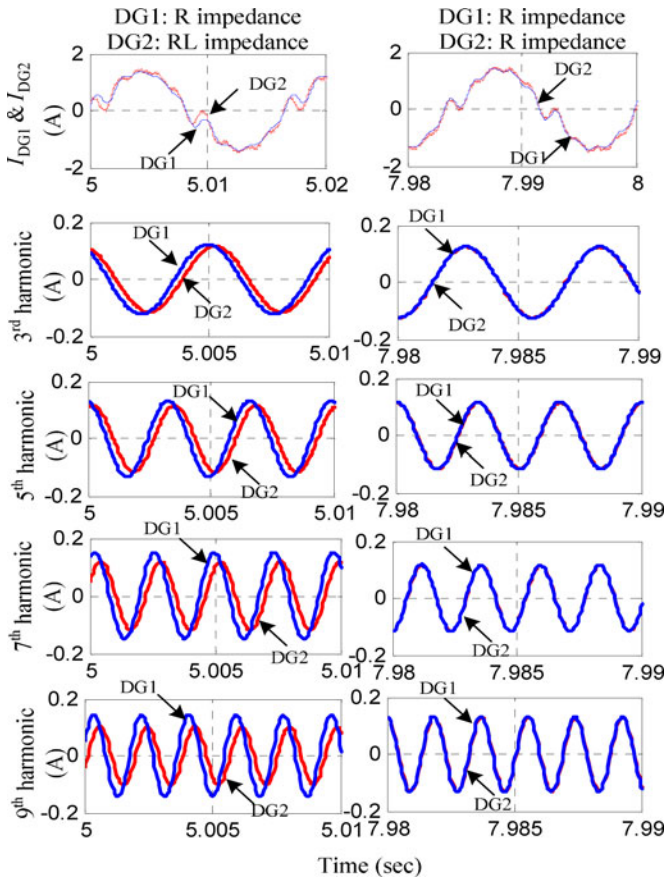

Fig. 15. DG unit 1 and DG unit 2 line currents and their harmonic components (grid-tied operation of two parallel DG units).

component of the proposed nonlinear virtual impedance is used to compensate the impact of DG unit *LCL* filter grid-side inductor. The resistive component is responsible for active damping. With properly controlled DG equivalent harmonic impedance at selected harmonic frequencies, the proposed method can also eliminate the harmonic circulating current among multiple DG units with mismatched output filter parameters. Comprehensive simulations are conducted to confirm the validity of the proposed method.

REFERENCES

[1] H. Akagi, "Active harmonic filters," *Proc. IEEE*, vol. 93, no. 12, pp. 2128–2141, Dec. 2005.

[2] H. Akagi, H. Fujita, and K. Wada, "A shunt active filter based on voltage detection for harmonic termination for radial power distribution system," *IEEE Trans. Ind. Appl.*, vol. 35, no. 4, pp. 682–690, Jul./Aug. 1995.

[3] K. Wada, H. Fujita, and H. Akagi, "Consideration of a shunt active filter based on voltage detection for installation on a long distribution feeder," *IEEE Trans. Ind. Appl.*, vol. 38, no. 4, pp. 1123–1130, Jul./Aug. 2002.

[4] P.-T. Cheng and T.-L. Lee, "Distributed active filter systems (DAFSs): A new approach to power system harmonics," *IEEE Trans. Ind. Appl.*, vol. 42, no. 5, pp. 1301–1309, Sep./Oct. 2006.

[5] T.-L. Lee and P.-T. Cheng, "Design of a new cooperative harmonic filtering strategy for distributed generation interface converters in an islanding network," *IEEE Trans. Power Electron.*, vol. 42, no. 5, pp. 1301–1309, Sep. 2007.

[6] T.-L. Lee, J.-C. Li, and P.-T. Cheng, "Discrete frequency-tuning active filter for power system harmonics," *IEEE Trans. Power Electron.*, vol. 24, no. 5, pp. 1209–1217, Apr. 2009.

[7] T.-L. Lee and S.-H. Hu, "Discrete frequency-tuning active filter to suppress harmonic resonances of closed-loop distribution power system," *IEEE Trans. Power Electron.*, vol. 26, no. 1, pp. 137–148, Dec. 2010.

[8] N. Pogaku and T. C. Green, "Harmonic mitigation throughout a distribution system: A distributed-generator-based solution," *IEE Proc. Gener. Transmiss. Distrib.*, vol. 153, no. 3, pp. 350–358, May 2006.

[9] C. J. Gajanayake, D. M. Vilathgamuwa, P. C. Loh, R. Teodorescu, and F. Blaabjerg, "Z-source-inverter-based flexible distributed generation system solution for grid power quality improvement," *IEEE Trans. Energy Convers.*, vol. 24, pp. 695–704, Sep. 2009.

[10] Y. W. Li, D. M. Vilathgamuwa, and P. C. Loh, "Design, analysis and real-time testing of a controller for multibus microgrid system," *IEEE Trans. Power Electron.*, vol. 19, no. 5, pp. 1195–1204, Sep. 2004.

[11] Q.-C. Zhong and G. Weiss, "Synchronverters: Inverters that mimic synchronous generators," *IEEE Trans. Ind. Electron.*, vol. 58, no. 4, pp. 1259–1267, Apr. 2011.

[12] J. He and Y. W. Li, "Analysis, design and implementation of virtual impedance for power electronics interfaced distributed generation," *IEEE Trans. Ind. Appl.*, vol. 47, no. 6, pp. 2525–2538, Nov./Dec. 2011.

[13] Y. W. Li and C. N. Kao, "An accurate power control strategy for power-electronics-interfaced distributed generation units operating in a low-voltage multibus microgrid," *IEEE Trans. Power Electron.*, vol. 24, no. 12, pp. 2977–2988, Dec. 2009.

[14] J. M. Guerrero, L. G. Vicuna, J. Matas, M. Castilla, and J. Miret, "Output impedance design of parallel-connected UPS inverters with wireless load sharing control," *IEEE Trans. Ind. Electron.*, vol. 52, no. 4, pp. 1126–1135, Aug. 2005.
[15] J. M. Guerrero, L. G. Vicuna, J. Matas, M. Castilla, and J. Miret, "A wireless controller to enhance dynamic performance of parallel inverters in distributed generation systems," *IEEE Trans. Power Electron.*, vol. 19, no. 4, pp. 1205–1213, Sep. 2004.
[16] J. M. Guerrero, J. C. Vasquez, J. Matas, L.G. de Vicuna, and M. Castilla, "Hierarchical control of droop-controlled AC and DC microgrids - A general approach toward standardization," *IEEE Trans. Ind. Electron.*, vol. 55, no. 1, pp. 158–172, Jan. 2011.
[17] J. He, Y. W. Li, and S. Munir, "A flexible harmonic control approach through voltage controlled DG-grid interfacing converters," *IEEE Trans. Ind. Electron.*, vol. 59, no. 1, pp. 444–455, Jan. 2012.
[18] K. De Brabandere, B. Bolsens, J. Van den key bus, and A. Woyte, "A voltage and frequency droop control method for parallel inverters," *IEEE Trans. Power Electron.*, vol. 22, no. 4, pp. 1107–1115, Jul. 2007.
[19] B. Kroposki, C. Pink, R. Deblasio, H. Thomas, M. Simoes, and P. K. Sen, "Benefits of power electronic interfaces for distributed energy systems," *IEEE Trans. Energy Convers.*, vol. 25, no. 3, pp. 901–908, Sep. 2010.
[20] S. Chakraborty and M. G. Simoes, "Experimental evaluation of active filtering in a single-phase high-frequency AC microgrid," *IEEE Trans. Energy Convers.*, vol. 24, no. 3, pp. 673–682, Sep. 2009.
[21] A. V. Timbus, R. Teodorescu, F. Blaabjerg, and U. Borup, "Online grid measurement and ENS detection for PV inverter running on highly inductive grid," *IEEE Power Electron. Lett.*, vol. 2, no. 3, pp. 77–82, Sep. 2004.
[22] C. J. Chou, Y. K. Wu, G. Y. Han, and C. Y. Lee, "Comparative evaluation of the HVDC and HVAC links integrated in a large offshore wind farm: An actual case study in Taiwan," *IEEE Trans. Ind. Appl.*, vol. 48, no. 5, pp. 1639–1648, Sep./Oct. 2008.
[23] C. C. Hsin and R. Bucknall, "Harmonic calculations of proximity effect on impedance characteristics in subsea power transmission cables," *IEEE Trans. Power Delivery.*, vol. 24, no. 4, pp. 2150–2158, Jul./Aug. 2009.

Jinwei He received the B.Eng. degree from Southeast University, Nanjing, China, in 2005; the M.Sc. degree from the Institute of Electrical Engineering, Chinese Academy of Sciences, Beijing, China, in 2008; and the Ph.D. degree from the University of Alberta, Edmonton, AB, Canada, in 2013, all in electrical engineering.

From 2008 to 2009, he was a Power Electronics Engineer with China Electronics Technology Group Corporation, Beijing. In 2012, he was a Visiting Scholar at the Institute of Energy Technology, Aalborg University, Aalborg, Denmark. Since 2013, he has been a Power Electronics Engineer at Accuenergy Canada Inc., Toronto, ON, Canada. His research interests include variable-frequency drive of railway traction motors, design of linear electric machine, power quality and active filters, and high-power electronics applications in distributed power generation and ground transportation.

Yun Wei Li (S'04–M'05–SM'11) received the B.Sc. degree in electrical engineering from Tianjin University, Tianjin, China, in 2002, and the Ph.D. degree in electrical engineering from Nanyang Technological University, Singapore, in 2006.

In 2005, he was a Visiting Scholar with Aalborg University, Aalborg, Denmark. From 2006 to 2007, he was a Postdoctoral Research Fellow at Ryerson University, Toronto, ON, Canada. In 2007, he was with Rockwell Automation Canada, Cambridge, ON and in the same year, he later joined the Department of Electrical and Computer Engineering, University of Alberta, Edmonton, AB, Canada, where he is currently an Associate Professor. His research interests include distributed generation, microgrid, renewable energy, high-power converters, and electric motor drives.

Dr. Li is currently an Associate Editor for the IEEE TRANSACTIONS ON POWER ELECTRONICS and the IEEE TRANSACTIONS ON INDUSTRIAL ELECTRONICS. He was a Guest Editor for the IEEE TRANSACTIONS ON INDUSTRIAL ELECTRONICS Special Session on Distributed Generation and Microgrids. He is the recipient of the 2013 Richard M. Bass Outstanding Young Power Electronics Engineer Award from the IEEE Power Electronics Society.

Ruiqi Wang received the B.Eng. degree in electrical engineering and the Ph.D. degree in power system engineering from Shandong University, Jinan, China, in 2006 and 2012, respectively.

He was a Visiting Student at the University of Alberta, Edomonton, AB, Canada, from 2011 to 2012. He is currently an Electrical Research Engineer at Shandong Electric Power Research Institute, State Grid Corporation of China, Beijing, China. His research interests include power electronics application in power systems, microgrid, distributed power generation, and modern power system control.

Chenghui Zhang received the Bachelor's degree and the Master's degree in automation engineering, and the Ph.D. degree in control theory and operational research from the Shandong University of Technology, Jinan, China, in 1985, 1988, and 2001, respectively.

In 1988, he joined Shandong University, where he is currently a Professor of the School of Control Science and Engineering, the Chief Manager of Power Electronic Energy-Saving Technology & Equipment Research Center of Education Ministry, is a Specially Invited Cheung Kong Scholar Professor by the China Ministry of Education, and a Taishan Scholar Special Adjunct Professor. He is also the Chief Expert of the National "863" high technological planning. His research interests include optimal control of engineering, power electronics and motor drives, energy-saving techniques, and time-delay systems.